THE JOURNAL OF PHYSICAL CHEMISTRY B

Article

pubs.acs.org/JPCB

Competition among Ca^{2+}, Mg^{2+}, and Na^+ for Model Ion Channel Selectivity Filters: Determinants of Ion Selectivity

Todor Dudev*,† and Carmay Lim*,†,‡

†Institute of Biomedical Sciences, Academia Sinica, Taipei 115, Taiwan

‡Department of Chemistry, National Tsing Hua University, Hsinchu 300, Taiwan

ABSTRACT: Because voltage-gated ion channels play critical biological roles, understanding how they can discriminate the native metal ion from rival cations in the milieu is of great interest. Although Ca^{2+}, Mg^{2+}, and Na^+ are present in comparable concentrations outside the cell, the factors governing the competition among these cations for the selectivity filter of voltage-gated Ca^{2+} ion channel remain unclear. Using density functional theory combined with continuum dielectric methods, we evaluate the effect of (1) the number, chemical type, and charge of the ligands lining the pore, (2) the pore's rigidity, size, symmetry, and solvent accessibility, and (3) the Ca^{2+} hydration number outside the selectivity filter on the competition among Ca^{2+}, Mg^{2+}, and Na^+ in model selectivity filters. The calculations show how the outcome of this competition depends on the interplay between electronic and solvation effects. Selectivity for monovalent Na^+ over divalent Ca^{2+}/Mg^{2+} is achieved when solvation effects outweigh electrostatic effects; thus filters comprising a few weak charge-donating groups such as Ser/Thr side chains, where electrostatic effects are relatively weak and are easily overcome by solvation effects, are Na^+-selective. In contrast, selectivity for divalent Ca^{2+}/Mg^{2+} over monovalent Na^+ is achieved when metal−ligand electrostatic effects outweigh solvation effects. The key differences in selectivity between Mg^{2+} and Ca^{2+} lie in the pore size, oligomericity, and solvent accessibility. The results, which are consistent with available experimental data, reveal how the structure and composition of the ion channel selectivity pore had adapted to the specific physicochemical properties of the native metal ion to enhance the competitiveness of the native metal toward rival cations.

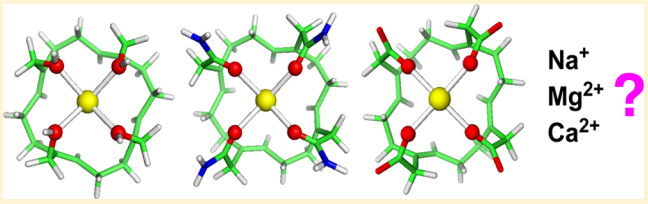

INTRODUCTION

Ion channels, specialized pore-forming proteins, are indispensable integral components of living cells and play a key role in regulating the cardiac, skeletal, and smooth muscle contraction, epithelial transport of nutrients and ions, hormone secretion, taste and pain sensation, and signal transduction.[1−3] Among these systems, the superfamily of voltage-gated (denoted by subscript v) sodium (Na_v), potassium (K_v), and calcium (Ca_v) channels found in excitable cells are of particular importance, as they control the cell action potential (by polarizing/depolarizing the cell membrane), muscular excitation/contraction, gene expression, and release of hormones and neurotransmitters. The three types of voltage-gated ion channels are characterized by remarkable metal selectivity allowing them to discriminate very efficiently between the "native" cation and competing metal ions from the cellular/extracellular milieu. Na_v channels exhibit a Na^+/K^+ selectivity ratio of ∼30:1,[4] while K_v channels are more discriminatory and select K^+ over Na^+ by a ratio of ∼1000:1.[2] Both monovalent ion channels are inaccessible to anions and exclude divalent cations.[2,5] The Ca_v channels are also highly discriminatory and select Ca^{2+} over Na^+ or K^+ by a ratio of over 1000:1[2,6] and do not conduct Mg^{2+}.[7] The metal ion selectivity of the channel is conferred by its selectivity filter—the *narrowest* part of the *open* pore. The selectivity filter is a mono-[4,8−16] or multilayered[17−20] ring-like structure (see Figure 1), lined with several metal-binding residues (e.g., Asp/Glu or Ser/Thr side chains and backbone carbonyl groups), donated by each of the channel pore-forming domains. The metal-ligating groups protrude toward the pore lumen and interact with the passing metal ion. The physical basis for metal selectivity in ion channels has been a subject of extensive investigations employing various experimental and theoretical methods, as summarized below for K_v, Na_v, and Ca_v channels.

X-ray structures of several K^+ channels[17−26] and insights from theoretical studies[27−42] have unraveled the key determinants of the K^+/Na^+ selectivity in K_v channels. The selectivity for K^+ over Na^+ in the selectivity filter is due to a relatively rigid, solvent-inaccessible pore lined with metal ligands that "over-coordinate" the small Na^+ and *not* to a rigid pore of exact geometry that fits only K^+ but not Na^+.[31,35−37,39] In the homotetrameric KcsA K^+ channel for example, the selectivity filter provides eight ligating backbone ligands (Figure 1a) and a low-dielectric medium, which favors octa-coordination/hydration of K^+; such an eight-fold coordination is further enforced by some form of rigidity from the protein matrix, which prohibits Na^+ from adopting a smaller coordination number, thus disfavoring Na^+ binding.[18,36,38−41]

Received: May 21, 2012
Revised: August 13, 2012
Published: August 13, 2012

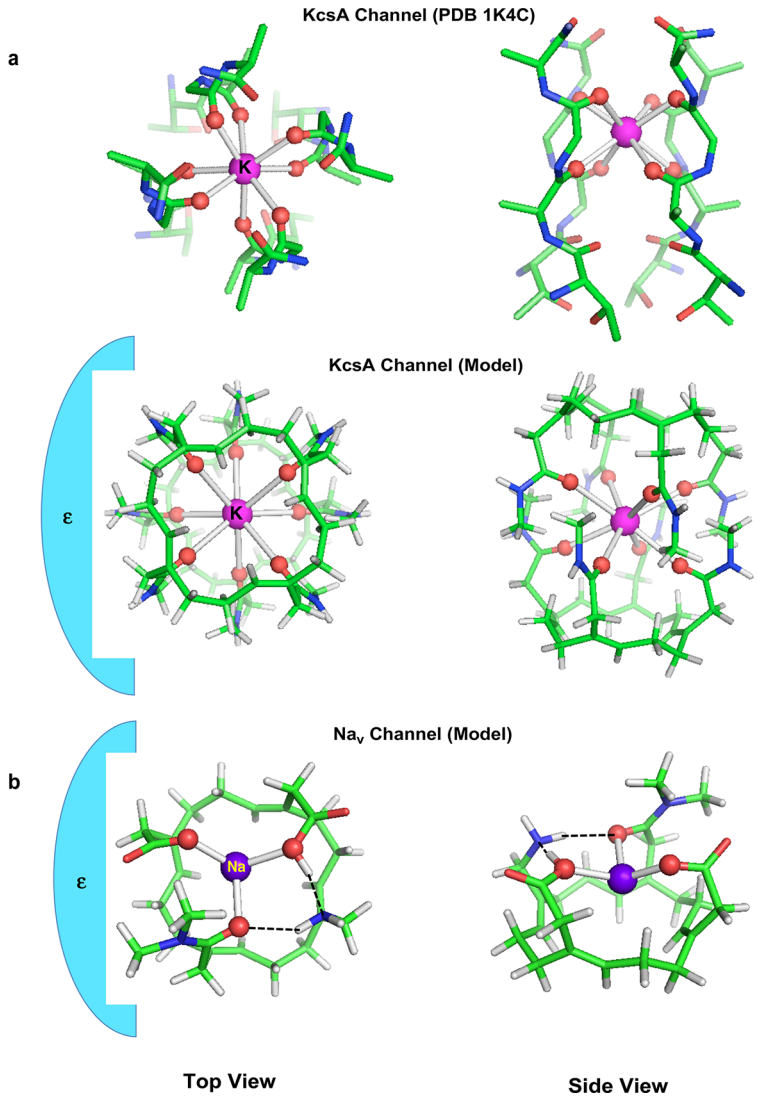

Figure 1. (a) PDB structure (ID 1k4c) of K^+ bound to eight backbone carbonyl groups in the homotetrameric KcsA channel selectivity filter modeled by K^+ bound to eight $-CONH_2$ attached to a carbon–hydrogen ring scaffold via methylene spacers with the rest of the filter represented by a continuum dielectric constant, ε; the fully optimized B3LYP/6-31+G(3d,p) structure taken from Dudev and Lim, 2009,[41] is shown. (b) Fully optimized B3LYP/6-31+G(3d,p) structure of Na^+-bound model DEKA selectivity filter taken from Dudev and Lim, 2010.[43]

Not surprisingly, factors favoring K^+/Na^+ selectivity in K^+ channels ("over-coordination" by backbone carbonyls) generally disfavor Na^+/K^+ selectivity in vertebrate Na_v channels with an asymmetric Asp-Glu-Lys-Ala (DEKA) selectivity filter. In the latter, the selectivity for Na^+ over K^+ is achieved by coordination to three strong charge-donating ligating groups (the Asp/Glu carboxylate oxygens and the Ala carbonyl oxygen; Figure 1b) lining a relatively narrow and rigid pore.[43] The conserved Lys comprising the DE**K**A motif does not bind the cation but helps to constrict and rigidify the pore by forming hydrogen bonds with the neighboring carbonyl and carboxylate oxygen atoms.[43] Notably, the pore's size/rigidity seems to be more important in determining ion selectivity in the DEKA filter of Na_v channels than in K_v channels, as a narrow and constricted pore in Na_v channels is more discriminative toward larger ions (K^+) than the larger aperture in K^+ channels is toward smaller ions (Na^+).[43]

The L-type Ca_v channel or homologues such as T-, N-, R-, and P/Q-type Ca_v channels control selective passage of Ca^{2+} from the *extra*cellular to *intra*cellular compartments along the concentration gradient. They preferably conduct extracellular Ca^{2+} (~1–3 mM[44,45]) against high background concentrations of other competing metal ions such as Na^+ (~150 mM[44]) and Mg^{2+} (~1 mM[44]). In addition, these Ca_v channels have to prevent *intra*cellular K^+ (~140 mM[44]) from passing in the opposite direction through the channel's pore. Although X-ray structures of Ca^{2+}-bound Ca_v channels are lacking, site-directed mutagenesis and channel-blocker binding experiments have determined the composition and oligomericity of several Ca_v channel selectivity filters.[12−14,46−52] Asp/Glu residues, whose side chains face the pore lumen, are found to line these filters. Notably, two Glu and two Asp residues (EEDD locus) line the selectivity filter of the *low* voltage-activated counterpart, while four Glu residues (EEEE locus) from four homologous domains comprise the selectivity filter of the *high* voltage-activated Ca_v channels. Interestingly, the alignment of the latter sequence with the bacterial Na_v channel selectivity filter sequence shows that the four Ca_v channel Glu residues align with the four Na_v channel Glu residues lining a short, water-filled selectivity filter in the 2.7 Å X-ray structure of a bacterial

dx.doi.org/10.1021/jp304925a | J. Phys. Chem. B 2012, 116, 10703−10714

Na_v channel captured in a closed-pore, metal-free conformation.[10]

In the absence of 3D structures, theoretical studies on the selectivity/permeability of Ca_v channels rely on models. Eisenberg and coauthors have modeled the selectivity filter as a cylindrical pore characterized by a given dielectric constant, the carboxylate groups of the EEEE/EEDD loci as eight mobile half-charged oxygens confined to the pore lumen but free to move inside, and metal cations as charged hard spheres with the respective crystal radii that interact with the filter's oxygens.[45,53−62] Monte Carlo simulations[45,56−60] on this model and calculations using the mean spherical approximation method[54,55,62] suggest that the Ca^{2+} versus Na^+ selectivity in Ca_v channels is governed primarily by the balance between the attractive cation−carboxylate electrostatic interactions and repulsive excluded volume of cations and carboxylates in the filter (charge-space competition); that is, the pore selects for Ca^{2+} as it provides more positive charge than Na^+ in the same volume to balance the negative charge of the carboxylate oxygens.[54,55,58] It is also affected by the pore radius and the protein dielectric constant: the Ca^{2+}/Na^+ selectivity increases when the pore radius and the protein dielectric constant decrease.[45,56,59]

A similar approach has been adopted by Corry and coworkers who have also modeled the Ca_v channel's selectivity filter as a narrow, cylindrical pore characterized by a given radius and dielectric constant. Unlike Eisenberg's model, the four Glu side chains were treated as four point charges of magnitude −0.811e placed at fixed positions inside the protein rather than as flexible units inside the filter, so they do not compete for space in the small volume of the pore.[32,34,63,64] Brownian dynamics simulations on this model indicate that Ca^{2+}/Na^+ selectivity is governed solely by the electrostatic interactions inside the channel pore and not by the cation's excluded volume or the filter's structure and volume.[32,34,64]

Lipkind and Fozzard[65] and Ramakrishnan et al.[66] have explicitly modeled the Ca_v channel's EEEE selectivity filter using the KcsA bacterial K^+ channel crystal structure and minimal β-barrel channel, respectively, as templates/scaffolds for anchoring the glutamates. Using molecular mechanics calculations with the consistent valence force field approximation, Lipkind and Fozzard[65] found that, in the absence of Ca^{2+}, the selectivity filter forms a wide, open pore (~6 Å) due to the repulsion among the negatively charged carboxylate groups lining the pore; upon Ca^{2+} binding, all four Glu side chains move to the center of the pore and directly interact with a single dehydrated Ca^{2+}.[65] Using molecular dynamics simulations with explicit water molecules, Ramakrishnan et al.[66] found that Ca^{2+} was more effective than Na^+ in competing for the selectivity filter, thus highlighting the role of electrostatic forces in controlling the pore selectivity/conductivity.[66]

In contrast to the above calculations using classical force fields, we have treated the metal ions and carboxylate ligands in the EEEE selectivity filter explicitly using density functional theory (DFT) to account for electronic effects such as polarization of the participating entities and charge transfer from the carboxylates to the metal cation, which cannot be accurately treated using classical force fields; the rest of the pore was represented by a continuum dielectric.[67] The calculations elucidate why selectivity filters with the same EEEE motif are Na^+-selective in bacterial Na_v channels but are Ca^{2+}-selective in high voltage-activated Ca_v channels. They suggest that the protein matrix, which can control the solvent accessibility, size, and relative rigidity of the selectivity filter, as well as the charge state of the metal ligands, is a key determinant of Ca^{2+} versus Na^+ selectivity in EEEE selectivity filters.

The aforementioned studies have focused on the competition between Ca^{2+} and Na^+ in the Ca_v channel's EEEE selectivity filter, while the rivalry between Ca^{2+} and other cations, particularly K^+ and Mg^{2+} that are present in high concentrations in the cellular/extracellular environment, has attracted little attention. While the determinants of the Ca^{2+}/K^+ selectivity are expected to be similar to that of the Ca^{2+}/Na^+ selectivity (both Na^+ and K^+ are univalent alkali ions with similar physicochemical properties), the factors governing the competition between Mg^{2+} and Ca^{2+} remain largely unknown. Several intriguing questions on the preference for Ca^{2+} over both Na^+ and Mg^{2+} in the Ca_v channel selectivity filters remain: (1) Do the factors favoring Ca^{2+} over Na^+ in the EEEE selectivity filter also favor Ca^{2+} over Mg^{2+}? (2) Is the four-carboxylate (EEEE/EEDD) filter in Ca_v channels the only motif that can discriminate efficiently Ca^{2+} from both Na^+ and Mg^{2+}? (3) Can filters lined with different numbers or types of metal-ligating groups also discriminate the native cation from competing ions in the milieu; that is, what is the role of the number, chemical type, and charge of the ligands lining the filter in the selectivity process? (4) Does the cation hydration inside and outside the filter affect the competition among Ca^{2+}, Mg^{2+}, and Na^+?

Herein, we address the above questions using DFT combined with continuum dielectric methods[41,43,68−71] to systematically evaluate how the competition among Ca^{2+}, Mg^{2+}, and Na^+ in model Ca_v selectivity filters depends on properties of (i) the metal cation—the number of water molecules bound directly to the metal; that is, the metal hydration number, outside the selectivity filter, (ii) the metal ligands—the number and chemical type/charge of the metal-ligating groups lining the selectivity filter, and (iii) the protein matrix—the pore's size, rigidity, solvent accessibility, and symmetry as well as the protonation state of the Asp/Glu ligands. Selectivity filters with metal-ligating groups differing in number (3, 4, or 5) and type/charge (−OH, $-CONH_2$, $-COO^-$) were modeled. The metal ions and first-shell ligands, which play a key role in the Ca^{2+}/Na^+ and Ca^{2+}/Mg^{2+} competition, were treated explicitly using DFT, while the region inside the selectivity filter was represented by a continuum dielectric varying from 4 to 30, mimicking binding sites of increasing solvent exposure (see Methods). The outcome of the competition between the bulk solvent and the protein ligands for the native cation in a Ca_v selectivity filter was assessed by computing the free energy for replacing Ca^{2+} bound inside the model selectivity filter, [Ca^{2+}-filter], with Na^+ or Mg^{2+}:

$$[M(H_2O)_6]^{q+} + [Ca^{2+}\text{-filter}] + n(H_2O) \rightarrow [M^{q+}\text{-filter}] + [Ca(H_2O)_{6+n}]^{2+} \quad (1)$$

In eq 1, M = Na or Mg, q = 1 for Na and 2 for Mg, and n = 0, 1, or 2 for hexa-, hepta-, and octahydrated Ca^{2+}, respectively. Hexahydrated Na^+ and Mg^{2+} were modeled, as the hydration number of Na^+ and Mg^{2+} is predominantly 6,[72,73] while Ca^{2+} hydrates were modeled as $[Ca(H_2O)_6]^{2+}$, $[Ca(H_2O)_7]^{2+}$, and $[Ca(H_2O)_8]^{2+}$ since the hydration number of Ca^{2+} varies from 6 to 8 with 7 appearing to be more common.[73] The ion

dx.doi.org/10.1021/jp304925a | J. Phys. Chem. B 2012, 116, 10703−10714

exchange free energy for eq 1 in an environment characterized by a dielectric constant $\varepsilon = x$ is given by,

$$\Delta G^x = \Delta G^1 + \Delta G_{solv}{}^x([M^{q+}\text{-filter}]) + \Delta G_{solv}{}^x([Ca(H_2O)_{6+n}]) - \Delta G_{solv}{}^x([Ca^{2+}\text{-filter}]) - \Delta G_{solv}{}^x([M(H_2O)_6]) - n\Delta G_{solv}{}^x(H_2O) \quad (2)$$

where ΔG^1 is the gas-phase free energy for eq 1, and $\Delta G_{solv}{}^x$ is the free energy for transferring a molecule in the gas phase to a medium characterized by dielectric constant $\varepsilon = x$. Positive ΔG^x values imply a Ca^{2+}-selective filter, whereas negative ΔG^x values imply a Na^+/Mg^{2+}-selective one. The aim of the calculations is to yield reliable trends in the free energy changes with varying parameters such as the solvent accessibility or size of the pore, rather than to reproduce the absolute metal exchange free energies in the selectivity filters. Notably, the methodology employed herein has yielded trends in the free energy changes in previous works[41,43,74−78] that are in line with experimental observations. The calculations reveal how nature, in response to the specific physicochemical properties of the native metal cation, had evolved the structure and composition of the ion channel selectivity filter to enhance selectivity for the native metal over rival ions from the surrounding fluids.

METHODS

Selectivity Filter Models Used and Justification. Unlike the KcsA K^+ channel selectivity filter, which comprises four tetrameric rings one on top of the other (see Figure 1a,b), the Ca_v channel EEEE filter corresponding to the narrowest part of the channel pore likely comprises a single tetrameric ring, as in the bacterial Na_v channel crystal structure,[10] which shows four acidic side chains lining the narrowest part of the ion conduction pathway. To determine whether the four-carboxylate filter in Ca_v channels is the only motif that can discriminate efficiently Ca^{2+} from Na^+ and Mg^{2+}, "symmetrical" filters containing various numbers of backbone carbonyl groups, Asp/Glu carboxylates, and Ser/Thr hydroxyl groups were modeled. (An asymmetrical pore lined with "mixed" metal-ligating groups, as shown in Figure 1b, has been studied in our previous work.[43]) The peptide backbone groups in the selectivity filters were modeled by $-CONH_2$, while the side chains of Ser/Thr were modeled by −OH and Asp/Glu by $-COO^-$. Models of trimeric, tetrameric, and pentameric ion channel selectivity filters were built using GaussView version 3.09,[79] following the guidelines from our previous work.[41] Different numbers (3, 4, or 5) of protein ligands were coordinated to the permeating ion (Na^+, Ca^{2+}, or Mg^{2+}) and attached to a carbon−hydrogen ring scaffold via methylene spacers (Figures 2−5).

Compared to earlier simplified models[31,33,36−38,53,63] used to study metal selectivity in ion channels, our augmented models bear closer resemblance to the channel's selectivity filter: (1) The ring mimics the oligomeric state and overall symmetry/asymmetry of the ion channel pore. (2) The ring scaffold prevents the metal ligands from drifting away or assuming unrealistic, pore-occluding positions during geometry optimization. (3) The metal-ligating groups and their connection to the ring are flexible enough to allow them to optimize their positions upon metal binding. (4) The shape and C−H orientations of the ring do not obstruct the pore lumen. (5) The ring's C−H chain length would not bias the results, as the number of carbon atoms in the trimeric ring is similar/equal to that in the tetrameric/pentameric ring.

Gas-Phase Free Energy Calculations. Among several combinations of different ab initio/DFT methods (HF, MP2, S-VWN, and B3-LYP) and basis sets (6-31+G(d,p), 6-31+G-(2d,2p), 6-31+G(3d,p), 6-31+G(3d,2p), 6-311++G(d,p), and 6-311++G(3df,3pd)), the B3-LYP/6-31+G(3d,p) method has been shown to be the most efficient in yielding dipole moments of the metal ligands that are closest to the respective experimental values; it can also reproduce (within experimental error) the metal−oxygen bond distances in aqua and crown−ether complexes, which resemble metal-occupied ion channel pores.[41] Hence, the B3-LYP/6-31+G(3d,p) method was used to optimize the geometry of each metal complex without any constraints and to compute the electronic energies, E_{el}, using the Gaussian 09 program.[80] Frequency calculations for each optimized structure were performed at the same level of theory. A few imaginary frequencies could not be eliminated in the optimized structures containing five −OH or $-COO^-$ groups bound to Mg^{2+} and Na^+; hence the ion exchange free energies (eq 1) in these pentameric filters were not computed. No imaginary frequency was found in the other optimized structures. The B3-LYP/6-31+G(3d,p) frequencies were scaled by an empirical factor of 0.9613[81] and used to compute the thermal energies including zero-point energy (E_{th}) and entropies (S). The differences ΔE_{el}, ΔE_{th}, ΔPV (work term), and ΔS between the products and reactants in eq 1 were used to calculate the gas-phase ΔG^1 free energy at T = 298.15 K according to:

$$\Delta G^1 = \Delta E_{el} + \Delta E_{th} + \Delta PV - T\Delta S \quad (3)$$

The basis set superposition error has been found to be negligible for the type of ion exchange reactions described by eq 1;[41] hence, it was not considered in the present calculations.

Solution Free Energy Calculations. The $\Delta G_{solv}{}^x$ were estimated by solving Poisson's equation using finite difference methods[82,83] with the MEAD (Macroscopic Electrostatics with Atomic Detail) program,[84] as described in previous works.[85] Natural bond orbital atomic charges, which are known to be numerically quite stable with respect to basis set changes,[86] were employed in the calculations. The effective solute radii were obtained by adjusting the CHARMM (version 22)[87] van der Waals radii to reproduce the experimental hydration free energies of Na^+, Mg^{2+}, Ca^{2+}, and model ligand molecules to within 1 kcal/mol (Table 1). The resulting values (in Å) are: R_{Na} = 1.72, R_{Mg} = 1.50, R_{Ca} = 1.75, R_C = 1.95, R_N = 1.75, $R_O(-CONH_2)$ = 1.72, $R_O(-CH_2OH)$ = 1.90, $R_O(H_2O/Na-H_2O)$ = 1.85, $R_O(Mg/Ca-H_2O)$ = 1.84, $R_O(Na-COO)$ = 1.40, $R_O(Mg-COO)$ = 1.34, $R_O(Ca-COO)$ = 1.25, R_H = 1.50, $R_H(H_2O-Na)$ = 1.26, $R_H(H_2O-Mg)$ = 1.125, $R_H(H_2O-Ca)$ = 1.053.

Solution Free Energy Calibrations. To ascertain the accuracy of the metal exchange free energy calculations in revealing reliable trends, we computed the ΔG[80] for replacing dihydrated Ca^{2+} bound to nitrilotriacetic acid (NTA) with Na^+ and Mg^{2+} in aqueous solution (see Table 1). The resulting ΔG[80] for $Na^+ \rightarrow Ca^{2+}$ exchange (6.7 kcal/mol) and $Mg^{2+} \rightarrow Ca^{2+}$ exchange (0.4 kcal/mol) are in close agreement with the respective experimental values (7.1 and 1.2 kcal/mol[88]).

Table 1. Comparison between Computed and Experimental Hydration Free Energies, ΔG_{solv}^{80}, of Metal Cations and Ligands, and Free Energies of Metal Exchange, ΔG_{ex}^{80}, in Nitrilotriacetic Acid (NTA) Complexes

	ΔG_{solv}^{80} (kcal/mol)		
metal or ligand	expt	calcd	error[a]
Na^+	−98.3[b]	−98.7	−0.4
Mg^{2+}	−455.5[b]	−456.3	−0.8
Ca^{2+}	−380.8[b]	−380.9[c]	−0.1[c]
		−381.1[d]	−0.3[d]
		−381.1[e]	−0.3[e]
H_2O	−6.3[f]	−6.7	−0.4
CH_3OH	−5.1[g]	−6.1	−1.0
$HCONH_2$	−10.0[h]	−10.6	−0.6
CH_3COO^-	−82.2[i]	−82.3	−0.1
reaction	ΔG_{ex}^{80} (kcal/mol)		
$[Na(H_2O)_6]^+ + H_2O + [Ca(H_2O)_2(NTA)]^- \rightarrow [Na(H_2O)_2(NTA)]^{2-} + [Ca(H_2O)_7]^{2+}$	7.1[j]	6.7	−0.4
$[Mg(H_2O)_6]^{2+} + H_2O + [Ca(H_2O)_2(NTA)]^- \rightarrow [Mg(H_2O)_2(NTA)]^- + [Ca(H_2O)_7]^{2+}$	1.2[j]	0.4	−0.8

[a]Error = ΔG^{80}(calcd) − ΔG^{80}(expt). [b]From Friedman and Krishnan, 1973.[89] [c]Hexahydrated Ca^{2+}. [d]Heptahydrated Ca^{2+}. [e]Octahydrated Ca^{2+}. [f]From Ben-Naim and Marcus, 1984.[90] [g]From Chambers et al., 1996.[91] [h]Experimental solvation free energy of $HCONH(CH_3)$ from Wolfenden et al., 1978.[92] [i]From Lim et al., 1991.[83] [j]Calculated from the experimental stability constants of the respective metal complexes from Smith and Martell, 1987;[88] NTA binds in a tetradentate fashion (including central N atom) to the metal.

RESULTS

Selectivity Filters Lined with Hydroxyl Groups. Selectivity filters comprising 3 and 4 OH-ligating groups (representing Ser/Thr side chains) were modeled. Figure 2a,b shows the respective structures (denoted as **3OH** and **4OH**)

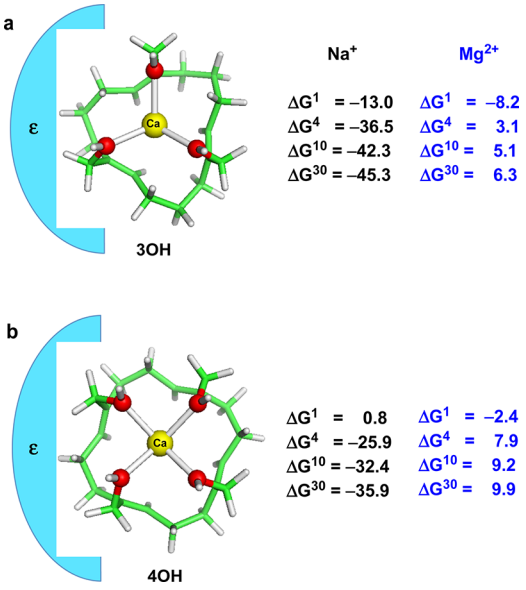

Figure 2. Fully optimized structures of Ca^{2+}-bound model selectivity filters comprising (a) 3 and (b) 4 OH-ligating groups (representing Ser/Thr side chains). The free energies ΔG^x (in kcal/mol) for replacing Ca^{2+} in the filter characterized by dielectric constant $\varepsilon = x$ with Na^+ or Mg^{2+} (eq 1 with $n = 1$) are shown on the left and right, respectively.

and the free energies ΔG^x for replacing Ca^{2+} with Na^+ or Mg^{2+} in the filter characterized by dielectric constant $\varepsilon = x$.

Ca^{2+} vs Na^+ Selectivity. The free energy for $[Na(H_2O)_6]^+ + [Ca\text{-filter}]^{2+} + H_2O \rightarrow [Na\text{-filter}]^+ + [Ca(H_2O)_7]^{2+}$ is a net result of electronic and solvation effects. In the gas phase where only electronic effects are present, the **3OH** filter selects Na^+ over Ca^{2+} (Figure 2, $\Delta G^1 = -13$ kcal/mol), because three hydroxyl oxygen atoms do not transfer enough charge to stabilize dicationic Ca^{2+} compared to monocationic Na^+. However, increasing the number of ligating hydroxyl oxygen atoms to four increases the net charge transfer to Ca^{2+} more than that to Na^+, thus stabilizing Ca^{2+} relative to Na^+, and ΔG^1 becomes slightly positive. Increasing the solvent accessibility of the filter ($x \geq 4$) enhances Na^+/Ca^{2+} selectivity (Figure 2, ΔG^x becomes more negative with increasing x), mainly because the free energy gain upon releasing Ca^{2+} from the filter outweighs the free energy loss upon Na^+ binding to the filter (see eq 1). Thus, selectivity filters lined with 3 or 4 Ser side chains are *not* selective for Ca^{2+} over Na^+ (Figure 2, negative ΔG^x, $x \geq 4$).

Ca^{2+} vs Mg^{2+} Selectivity. Electronic and solvation effects have opposite effects on the free energy for $[Mg(H_2O)_6]^{2+} + [Ca\text{-filter}]^{2+} + H_2O \rightarrow [Mg\text{-filter}]^{2+} + [Ca(H_2O)_7]^{2+}$. Electronic effects favor Mg^{2+} over Ca^{2+} in the **3OH** and **4OH** filters (Figure 2, negative ΔG^1), because Mg^{2+} is a better electron acceptor (Lewis acid) than Ca^{2+} and has more favorable electrostatic interactions with the hydroxyl oxygen atoms than Ca^{2+} in the gas phase. Compared to the **3OH** filter (Figure 2a, $\Delta G^1 = -8$ kcal/mol), the Mg^{2+}/Ca^{2+} selectivity in the **4OH** filter is diminished (Figure 2b, $\Delta G^1 = -2$ kcal/mol), largely because the repulsion among four hydroxyl oxygen atoms bound to Mg^{2+} is greater than that around the larger Ca^{2+}. Solvation effects, however, favor Ca^{2+} over Mg^{2+} due mainly to the higher desolvation penalty of the incoming Mg^{2+} compared to the solvation free energy gain of the outgoing Ca^{2+} (Figure 2, positive ΔG^x, $x \geq 4$). Thus, increasing the solvent exposure and oligomericity of the pore enhance the selectivity for Ca^{2+} over Mg^{2+}.

Selectivity Filters Lined with Amide Groups. The key difference between carbonyl and hydroxyl oxygen atoms as metal ligands lies in their charge-donating ability: the carbonyl group has a larger dipole moment and a stronger charge-donating ability than the hydroxyl group.[27,71] Compared to the **3OH** and **4OH** selectivity filters, the respective **3CONH$_2$** (Figure 3a) and **4CONH$_2$** (Figure 3b) filters are more selective for the better electron-accepting cation in the gas phase, favoring Ca^{2+} over Na^+ (ΔG^1 is more positive than that in Figure 2) and Mg^{2+} over Ca^{2+} (ΔG^1 is more negative than that in Figure 2). As for the **3OH** and **4OH** filters, solvation effects dominate and favor the incoming cation with the smaller desolvation penalty; i.e., Na^+ over Ca^{2+} and Ca^{2+} over Mg^{2+}. However, because of the larger electronic effects (larger absolute $|\Delta G^1|$), the **3CONH$_2$** and **4CONH$_2$** filters exhibit weaker Na^+/Ca^{2+} selectivity (ΔG^x, $x \geq 4$, is less negative) and Ca^{2+}/Mg^{2+} selectivity (ΔG^x, $x \geq 4$, is less positive) compared to the **3OH** and **4OH** filters.

Increasing the number of amide-ligating groups further enhances electronic effects, which dictate ion selectivity for solvent-*inaccessible* filters lined with ≥5 backbone amide groups, favoring Ca^{2+} over Na^+ and Mg^{2+} (Figure 3c, positive ΔG^x, $x \leq 4$). This is because increasing the number of amide-ligating groups increases the net charge transferred to the metal cation and steric/electronic repulsion among the carbonyl oxygen atoms. Since Ca^{2+} and Na^+ have similar ionic radii (~1 Å for

dx.doi.org/10.1021/jp304925a | J. Phys. Chem. B 2012, 116, 10703−10714

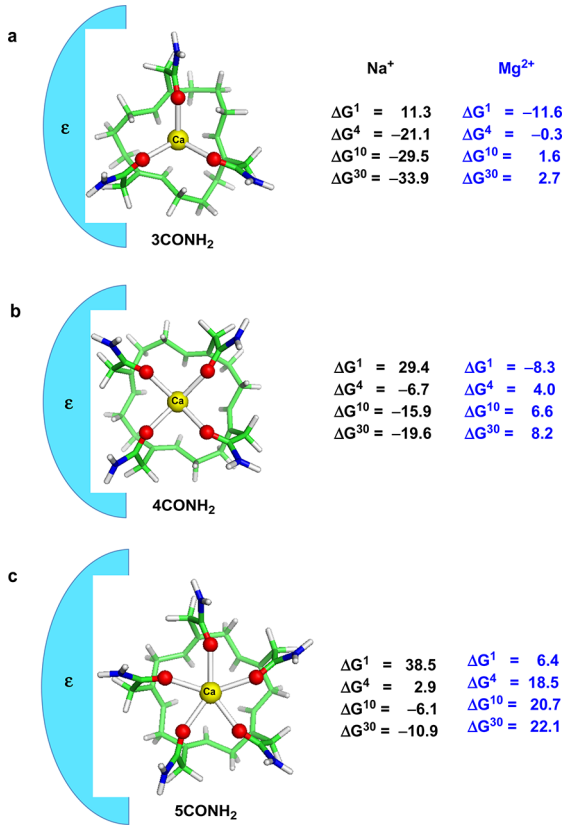

Figure 3. Fully optimized structures of Ca^{2+}-bound model selectivity filters comprising (a) 3, (b) 4, and (c) 5 $CONH_2$-ligating groups (representing peptide backbone groups). The free energies ΔG^x (in kcal/mol) for replacing Ca^{2+} in the filter characterized by dielectric constant $\varepsilon = x$ with Na^+ or Mg^{2+} (eq 1 with $n = 1$) are shown on the left and right, respectively.

hexacoordination), but Ca^{2+} has stronger electrostatic interactions with five carbonyl oxygen atoms lining the filter than Na^+, substitution by Na^+ is strongly disfavored ($\Delta G^1 = 39$ kcal/mol). On the other hand, Mg^{2+} (with an ionic radius of 0.72 Å) is significantly smaller than Ca^{2+}; thus repulsion among five or more carbonyl oxygen atoms bound to the small Mg^{2+} is greater than that around the larger Ca^{2+}, prohibiting substitution by Mg^{2+} ($\Delta G^1 = 6.4$ kcal/mol). Increasing solvent exposure of the pentameric filter in Figure 3c reverses the Ca^{2+}/Na^+ selectivity, favoring Na^+ over Ca^{2+} in a solvent-accessible pore (negative ΔG^x, $x \geq 10$), but enhances Ca^{2+}/Mg^{2+} selectivity (positive ΔG^x, $x \geq 4$).

Selectivity Filters Comprising Carboxylate Groups. Compared to the neutral carbonyl and hydroxyl ligands, the negatively charged carboxylate has far stronger charge-donating ability and favors the better Lewis acid cation in tri/tetrameric filters: Ca^{2+} over Na^+ and Mg^{2+} over Ca^{2+} (Figure 4a,b). The carboxylate's strong charge-donating ability affects the competition between cations in different oxidation states (Ca^{2+} and Na^+) more than that between cations of the same charge (Ca^{2+} and Mg^{2+}), as evidenced by the gas-phase free energies. For example, the ΔG^1 for replacing Ca^{2+} with Na^+ in the **3COO$^-$** filter (218 kcal/mol) is an order of magnitude more positive than that in the **3CONH$_2$** filter (11 kcal/mol), whereas the ΔG^1 values for replacing Ca^{2+} with Mg^{2+} in the **3COO$^-$** (−25 kcal/mol) and **3CONH$_2$** (−12 kcal/mol) filters are of the same order of magnitude. Hence, the ΔG^1 for replacing Ca^{2+} with Na^+ in the **3COO$^-$** and **4COO$^-$** filters can overcome solvation effects, favoring Ca^{2+} over Na^+ (Figure 4a,b, positive ΔG^x, $x \geq 4$). The selectivity for Ca^{2+} over Na^+ and Mg^{2+} is enhanced if the carboxylate filter provides four rather than three carboxylates.

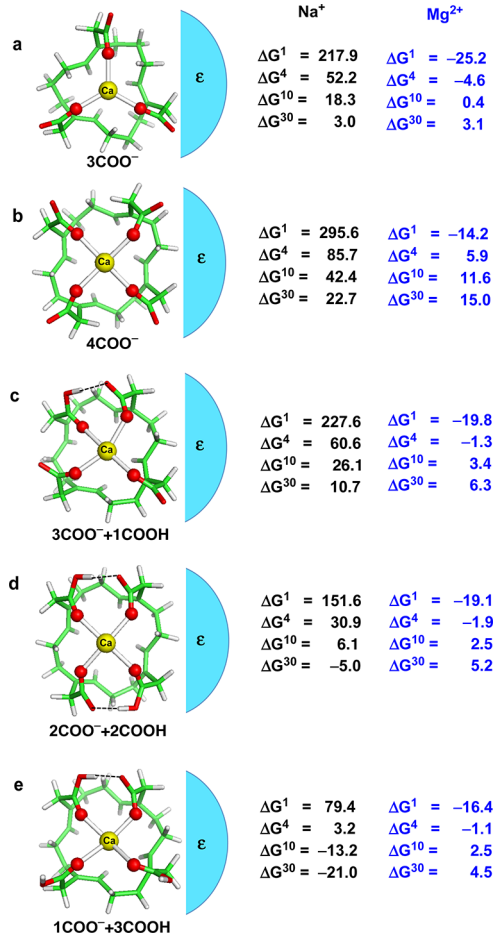

Figure 4. Fully optimized structures of Ca^{2+}-bound model selectivity filters comprising (a) 3 and (b) 4 COO^--ligating groups (representing negatively charged Asp/Glu side chains) and the model EEEE filter with (c) 1, (d) 2, and (e) 3 of the carboxylates protonated. The free energies ΔG^x (in kcal/mol) for replacing Ca^{2+} in the filter characterized by dielectric constant $\varepsilon = x$ with Na^+ or Mg^{2+} (eq 1 with $n = 1$) are shown on the left and right, respectively.

Dependence on the Asp/Glu Protonation State. The protein matrix may affect the carboxylate protonation state of Asp/Glu lining a selectivity filter. To assess the effect of the Asp/Glu protonation state on ion selectivity, we computed the free energies for replacing Ca^{2+} with Na^+/Mg^{2+} in tetrameric selectivity filters comprising varying numbers of deprotonated and protonated carboxylate groups (see Figures 4c–e).

Ca^{2+} vs Na^+ Selectivity. Protonation of carboxylate ligand(s) reduces the Ca^{2+}/Na^+ selectivity. The gas-phase ΔG^1 for replacing Ca^{2+} with Na^+ in the **4COO$^-$** filter (296 kcal/mol) decreases sharply to 228, 152, and 79 kcal/mol in the **3COO$^-$ + 1COOH** (Figure 4c), **2COO$^-$ + 2COOH** (Figure 4d), and **1COO$^-$ + 3COOH** (Figure 4e) filter, respectively. This is because reducing the number of $-COO^-$ groups attenuates the favorable electrostatic interactions with dicationic Ca^{2+} more than that with monocationic Na^+. Solvation effects further attenuate the ΔG^1 yielding lower positive or negative ΔG^x; hence, *solvent-accessible* selectivity filters with one or two

dx.doi.org/10.1021/jp304925a | J. Phys. Chem. B 2012, 116, 10703−10714

carboxylates are selective for Na^+ over Ca^{2+} (Figure 4d/e, negative ΔG^{30}).

Ca^{2+} vs Mg^{2+} Selectivity. Protonation of carboxylate groups affects the competition between Ca^{2+} and Mg^{2+} to a lesser extent than that between Ca^{2+} and Na^+: Upon protonation of 1−3 carboxylate ligands in the **4COO$^-$** filter, the ΔG^1 for replacing Ca^{2+} with Mg^{2+} decreases by 2−6 kcal/mol, whereas the ΔG^1 for replacing Ca^{2+} with Na^+ decreases by 68−216 kcal/mol. Notably, the **3COO$^-$ + 1COOH** filter has a less favorable ΔG^1 (−20 kcal/mol) than the **3COO$^-$** filter (−25 kcal/mol), as the extra −COOH group increases steric repulsion among the oxygen atoms around Mg^{2+} compared to the larger Ca^{2+}; however, it has a more favorable ΔG^1 than the **4COO$^-$** filter (Figure 4b, −14 kcal/mol), as protonation of one of the carboxylates reduces the ligand−ligand repulsion in the Mg^{2+} complex relative to the Ca^{2+} counterpart. Consequently, protonation of one or more carboxylates in the **4COO$^-$** filter abolishes or reduces the Ca^{2+}/Mg^{2+} selectivity.

Dependence on the Pore Size. The size of its pore would affect the direct interaction between the metal ion and its ligand; in a sufficiently large pore, the metal cation may not be able to bind a ligand directly but may do so indirectly via its bound water. To assess how ion selectivity depends on the degree of metal hydration inside the filter, we computed the free energies for replacing Ca^{2+} with Na^+/Mg^{2+} in filters lined with 4 $-COO^-$ groups where the metal ion retains 1, 2, or 4 of its first-shell water molecules. Increasing the number of metal-bound water molecules in the filter strongly impacts Ca^{2+}/Na^+ and Ca^{2+}/Mg^{2+} selectivity.

Ca^{2+} vs Na^+ Selectivity. A narrow pore that dehydrates the passing cation favors Ca^{2+} over Na^+ (Figure 5a, large positive ΔG^x). Increasing metal hydration reduces the Ca^{2+}/Na^+ selectivity: The gas-phase ΔG^1 becomes less positive because a water molecule bridging the metal cation and the carboxylate ligand results in longer metal−O(carboxylate) distance, which disfavors Ca^{2+} binding more than Na^+ binding.[67] Increasing the solvent exposure of the pore further reduces the Ca^{2+}/Na^+ selectivity. Hence, solvent-accessible selectivity filters that can accommodate the metal with two or more water ligands favor Na^+ over Ca^{2+}: ΔG^{30} = −2 kcal/mol for dihydrated ions (Figure 5c) and −6 kcal/mol for tetrahydrated ions (Figure 5d).

Ca^{2+} vs Mg^{2+} Selectivity. Increasing metal hydration favors Mg^{2+} over Ca^{2+}: The gas-phase ΔG^1 values for the hydrated structures (Figures 5b−d) are more negative than the ΔG^1 for dehydrated **4COO$^-$**. This is because Mg^{2+}, being a stronger Lewis acid than Ca^{2+}, polarizes the metal−bound water molecule(s) to a greater extent; thus the metal−water and water−carboxylate interactions are stronger for Mg^{2+} than for Ca^{2+}. Relative to the **4COO$^-$** filter, the decreased ΔG^1 upon metal hydration results in less positive ΔG^x ($x \geq 10$) for the **4COO$^-$/1W** (Figure 5b) filter and negative ΔG^x ($x \geq 4$) for the **4COO$^-$/2W** (Figure 5c) and the **4COO$^-$/4W** (Figure 5d) filters. Hence, a solvent-accessible filter that fits monohydrated metal ions is still Ca^{2+}-selective, whereas larger pores that accommodate the permeating cation bound to two or more water molecules select Mg^{2+} instead of Ca^{2+}.

Dependence on the Pore's Rigidity. To assess the strength of the effect of the selectivity filter's rigidity on metal competition, we computed the binding energies of *rival* Na^+ and Mg^{2+} ions bound to a **4COO$^-$** selectivity filter designed to fit the *native* Ca^{2+} (Figure 5a). The Ca^{2+}-bound **4COO$^-$** structure was fully optimized, and Ca^{2+} was replaced with Na^+/Mg^{2+}; the resultant structures were subjected to single-point energy calculations. The larger electronic energies of these nonoptimized Na^+- and Mg^{2+}-bound structures compared to those of the respective fully optimized Na^+ and Mg^{2+}-bound structures increases the energy for replacing Ca^{2+} with Na^+ by ∼6 kcal/mol and Mg^{2+} by ∼28 kcal/mol. This procedure was repeated with a larger pore that can accommodate a monohydrated metal ion (Figure 5b, **4COO$^-$/1W**). The energies exhibit a similar trend of changes as observed for the **4COO$^-$** structure: Substituting the *native* monohydrated Ca^{2+} with monohydrated Na^+ and Mg^{2+} increases the free energy of the metal exchange by ∼11 and ∼27 kcal/mol, respectively. Hence, rigidifying the EEEE/EEDD selectivity filter seems to be another means of increasing the selectivity for Ca^{2+} over Na^+ and especially Mg^{2+} in Ca_v channels. The energy cost for replacing Ca^{2+} with Mg^{2+} in a Ca^{2+}-optimized **4COO$^-$** filter is much higher than that for replacing Ca^{2+} with Na^+, mainly because the ionic size difference between Mg^{2+} and Ca^{2+} (0.28 Å for hexacoordination[93]) is greater than that between Na^+ and Ca^{2+} (0.02 Å[93]). This is reflected by the larger metal−O(carboxylate) distance difference between the optimized and the nonoptimized $[Mg\text{-filter4-}(COO)_4]^{2-}$ complexes (−0.28 Å) relative to that between the optimized and the non-optimized $[Na\text{-filter4-}(COO)_4]^{3-}$ counterparts (0.18 Å).

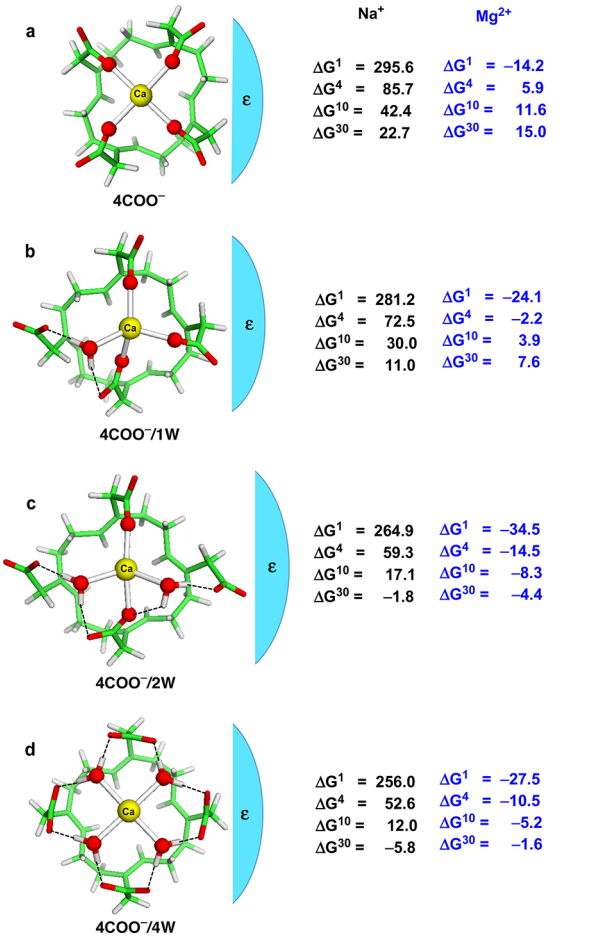

Figure 5. Fully optimized structures of Ca^{2+}-bound model EEEE selectivity filters with the metal bound with (a) 0, (b) 1, (c) 2, and (d) 4 water molecules. The free energies ΔG^x (in kcal/mol) for replacing Ca^{2+} in the filter characterized by dielectric constant $\varepsilon = x$ with Na^+ or Mg^{2+} (eq 1 with $n = 1$) are shown on the left and right, respectively.

dx.doi.org/10.1021/jp304925a | J. Phys. Chem. B 2012, 116, 10703−10714

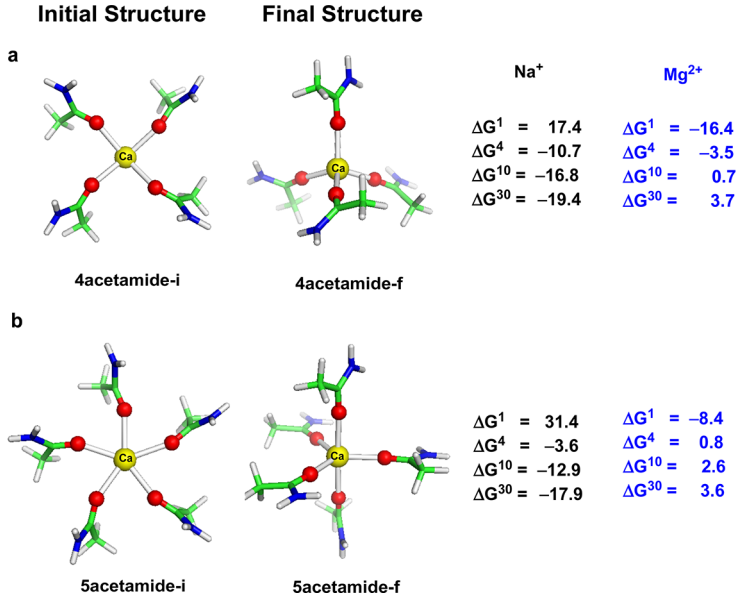

Figure 6. Initial planar and fully optimized structures of Ca^{2+} bound to (a) four and (b) five acetamide molecules. The free energies ΔG^x (in kcal/mol) for replacing Ca^{2+} in the complex characterized by dielectric constant $\varepsilon = x$ with Na^+ or Mg^{2+} are shown on the left and right, respectively.

Table 2. Calculated Enthalpies, Entropies, and Free Energies (in kcal/mol) of Ion Selectivity for $[\text{filter4-(COO)}_4]^{4-}$ in Media of Varying Dielectric Constants

reaction[a]	ΔH^1	$T\Delta S^1$	ΔG^1	ΔG^4	ΔG^{10}	ΔG^{30}
1. $[NaW_6]^+ + [\text{Ca-filter4-(COO)}_4]^{2-} \rightarrow [\text{Na-filter4-(COO)}_4]^{3-} + [CaW_6]^{2+}$	303.5	0.3	303.2	83.4	37.6	16.4
2. $[NaW_6]^+ + [\text{Ca-filter4-(COO)}_4]^{2-} + W \rightarrow [\text{Na-filter4-(COO)}_4]^{3-} + [CaW_7]^{2+}$	289.5	−6.1	295.6	85.7	42.4	22.7
3. $[NaW_6]^+ + [\text{Ca-filter4-(COO)}_4]^{2-} + 2W \rightarrow [\text{Na-filter4-(COO)}_4]^{3-} + [CaW_8]^{2+}$	276.0	−15.6	291.6	89.4	48.0	28.9
4. $[MgW_6]^{2+} + [\text{Ca-filter4-(COO)}_4]^{2-} \rightarrow [\text{Mg-filter4-(COO)}_4]^{2-} + [CaW_6]^{2+}$	−4.5	2.1	−6.6	3.6	6.8	8.7
5. $[MgW_6]^{2+} + [\text{Ca-filter4-(COO)}_4]^{2-} + W \rightarrow [\text{Mg-filter4-(COO)}_4]^{2-} + [CaW_7]^{2+}$	−18.5	−4.3	−14.2	5.9	11.6	15.0
6. $[MgW_6]^{2+} + [\text{Ca-filter4-(COO)}_4]^{2-} + 2W \rightarrow [\text{Mg-filter4-(COO)}_4]^{2-} + [CaW_8]^{2+}$	−32.0	−13.8	−18.2	9.5	17.1	21.1

[a]W denotes a water molecule. Solvation free energies (in kcal/mol) employed for the free water molecule are $\Delta G_{solv}{}^4 = -3.9$, $\Delta G_{solv}{}^{10} = -5.4$, and $\Delta G_{solv}{}^{30} = -6.4$.

To assess if the Ca^{2+}-selective **4COO$^-$** and **4COO$^-$/1W** filters exhibit the experimentally observed high Na^+/K^+ selectivity in the absence of Ca^{2+}, we replaced Ca^{2+} in the Ca^{2+}-optimized **4COO$^-$** and **4COO$^-$/1W** filters by K^+ and computed the single-point energies. Based on the electronic energies of the nonoptimized K^+ and Na^+-bound structures, the energy for $[Na(H_2O)_6]^+ + [\text{K-filter}]^{3-} \rightarrow [\text{Na-filter}]^{3-} + [K(H_2O)_6]^+$ is −28.2 kcal/mol for the **4COO$^-$** filter and −31.3 kcal/mol for the **4COO$^-$/1W** filter. The highly negative energies indicate that in the absence of Ca^{2+}, the channel is Na^+-selective, as the larger K^+ with less charge density misfits the Ca^{2+}-optimized pore more than Na^+.

Effect of the Pores' Imposed Symmetry. Due to the symmetry constraints imposed by the protein matrix, the ligands lining the selectivity filter bind the metal cation roughly in-plane (pseudo C_3, C_4, and C_5 symmetry for the metal-bound tri, tetra, and pentameric filters, respectively). While three ligands would favor coplanar binding of a metal ion,[94,95] would four or five ligands also favor near in-plane binding of a metal ion? To address this question, the metal-bound amides in **4CONH$_2$** (Figure 3b) and **5CONH$_2$** (Figure 3c) were detached from the ring scaffold. The resulting metal−acetamide complexes, denoted as **4acetamide-i** and **5acetamide-i** (Figure 6), were fully optimized. The initial planar structures were unstable and isomerized to energetically more favorable tetrahedral (**4acetamide-f**) and trigonal-bipyramidal (**5acetamide-f**) structures during optimization. Although the final structures are more stable than the initial ones, they have lost their pore-like shape, as one or two ligands have positioned themselves along the ion permeation pathway, thus occluding the pore and inhibiting ion conduction. This shows that the protein matrix plays an important role in properly orienting the metal-ligating groups so that they can interact with the passing cation, albeit with some "coordination strain", without obstructing the permeation pathway.

A comparison of the free energies for replacing Ca^{2+} with Na^+ or Mg^{2+} in **4acetamide-f** and **5acetamide-f** (Figure 6) with those in **4CONH$_2$** and **5CONH$_2$** (Figure 3) shows that freeing the metal-ligating groups from the selectivity filter scaffold results in increased Na^+/Ca^{2+} and decreased Ca^{2+}/Mg^{2+} selectivity: The gas-phase ΔG^1 for replacing Ca^{2+} with Na^+ decreases from 29 kcal/mol in **4CONH$_2$** to 17 kcal/mol in **4acetamide-f** and from 39 kcal/mol in **5CONH$_2$** to 31 kcal/mol in **5acetamide-f**. Likewise, the ΔG^1 for replacing Ca^{2+} with Mg^{2+} decreases from −8 kcal/mol in **4CONH$_2$** to −16 kcal/mol in **4acetamide-f** and from 6 kcal/mol in **5CONH$_2$** to −8 kcal/mol in **5acetamide-f**. The ΔG^x ($x < 30$) values follow the same trend. Hence, compared to the "planar" **4CONH$_2$** and **5CONH$_2$** structures, the respective tetrahedral (**4acetamide-f**) and trigonal-bipyramidal (**5acetamide-f**) geometries favor Na^+ and Mg^{2+} binding to a larger extent than Ca^{2+} binding. These calculations imply that the protein matrix enhances the

dx.doi.org/10.1021/jp304925a | J. Phys. Chem. B 2012, 116, 10703−10714

selectivity of Ca^{2+} over Na^+ or Mg^{2+} by imposing a planar-like symmetry on the metal ligands lining the selectivity filter.

Dependence on the Ca^{2+} Hydration Number. Although the most common hydration number from crystal structures of Ca^{2+} aqua complexes is seven, hydration numbers of six and eight have also been observed in a few structures. Thus, we evaluated the effect of the Ca^{2+} hydration number on ion selectivity of the channel's selectivity filter by computing the metal exchange free energies in the **4COO$^-$** filter where the outgoing Ca^{2+} is bound to six, seven, or eight water molecules (see Table 2). Increasing the Ca^{2+} hydration number increases the selectivity of the pore for Ca^{2+} over Na^+ and Mg^{2+} in a protein environment. When the hydration number of the Ca^{2+} increases from six to eight in a solvent−exposed filter, the ΔG^{30} for replacing Ca^{2+} with Na^+/Mg^{2+} increases from 16/9 kcal/mol in releasing hexahydrated Ca^{2+} to 29/21 kcal/mol in releasing octahydrated Ca^{2+}. This implies that the selectivity for Ca^{2+} over Na^+ and Mg^{2+} increases if more water molecules are bound to Ca^{2+} in the pore's vicinity and are freed when Ca^{2+} becomes bound to the selectivity filter.

DISCUSSION

Assessment of Errors. Systematic errors in the computed gas-phase and solvation free energies of the reactants are likely to partially cancel those of the respective products (see eq 2). Furthermore, errors in the gas-phase energies have been minimized by choosing the method/basis set that can yield experimental dipole moments of the metal ligands and metal−ligand distances, whereas errors in the solvation free energies have been minimized by calibrating the atomic radii to reproduce the experimental hydration free energies of the metal cations and ligands (see Table 1). The combined DFT/continuum dielectric approach was further validated: It yielded experimental free energies for replacing dihydrated Ca^{2+} bound to nitrilotriacetic acid with Na^+ and Mg^{2+} in water to within 1 kcal/mol (Table 1). Compared to the errors in the free energy computed in pure water, those evaluated for a lower dielectric medium, typical of metal-binding sites in proteins, would be expected to be smaller due to the decreased magnitude in the solvation free energies.[96] For example, the experimental solvation free energy of water is −6.3 kcal/mol[90] in water (x = 80), −5.7 kcal/mol[97] in 2-butanol solution (x = 16), and −3.9 kcal/mol[97] in ethyl ether solution (x = 4), while the respective computed values are −6.7, −5.9, and −4.0 kcal/mol, so the error decreases in magnitude from 0.4 kcal/mol at x = 80, to 0.2 kcal/mol at x = 16, to 0.1 kcal/mol at x = 4.

To assess the magnitude of the effect of distant nonbonding interactions between the ion/metal ligand and the rest of the protein on the metal−metal competition, the ring, which can be considered as the second metal coordination shell, was removed in the **4COO$^-$** filter (Figure 4b), leaving the metal ion bound to four CH_3COO^- ligands. Single-point energy calculations on these metal complexes were used to evaluate the gas-phase energy for eq 1. In the absence of nonbonding interactions between the metal ion/carboxylates and second-shell atoms, the gas-phase energy for replacing Ca^{2+} with Na^+ in the **4COO$^-$** filter (289.9 kcal/mol) increased by 5.4 to 295.3 kcal/mol, whereas that for replacing Ca^{2+} with Mg^{2+} (−19.5 kcal/mol) decreased by 0.4 to −19.9 kcal/mol. Thus, interactions between the metal and its ligands with the second shell contribute ∼2% to the metal-exchange energy in the **4COO$^-$** filter; more distant interactions in the channel protein are expected to contribute even less than those from the second shell atoms.

In interpreting the results, we focus on the trends of changes in the $Na^+ \rightarrow Ca^{2+}$ and $Mg^{2+} \rightarrow Ca^{2+}$ exchange free energies with varying molecular parameters. This would hopefully further cancel out systematic errors by comparing two metal exchange free energies. The reliability of the trends in the free energy changes was ultimately judged by comparing the findings obtained with available experimental data (see below).

Factors Controlling Ion Selectivity. The results herein show how the outcome of the competition between the native metal and the other cations present in comparable concentrations in the milieu depends on the properties of the protein (the pore's oligomericity, size, rigidity, symmetry, and solvent accessibility), the metal ligands (charge-donating ability), and the metal cation itself (size, charge-accepting ability, and hydration number). They also predict the types of filters that favor Ca^{2+}, Na^+, or Mg^{2+}. If the free energies for replacing Ca^{2+} in a given filter (Figures 2−6) with Na^+ and Mg^{2+} are positive, the filter is predicted to be Ca^{2+}-selective. If the $Na^+ \rightarrow Ca^{2+}$ ΔG^x is negative, but the $Mg^{2+} \rightarrow Ca^{2+}$ ΔG^x is less negative or positive, the filter is predicted to be Na^+-selective. Conversely, if the $Mg^{2+} \rightarrow Ca^{2+}$ ΔG^x is negative, but the $Na^+ \rightarrow Ca^{2+}$ ΔG^x is less negative or positive, the filter is predicted to be Mg^{2+}-selective.

Ca^{2+} Selectivity. The channel's selectivity for Ca^{2+} over Na^+ and Mg^{2+} generally increases when (i) the protein's oligomericity increases, (ii) the selectivity filter's rigidity increases, but its pore size decreases, (iii) the ligands lining the selectivity filter are anionic as opposed to neutral, and (iv) the Ca^{2+} hydration number *outside* the filter increases. However, increasing the solvent exposure of the pore reduces/reverses Ca^{2+}/Na^+ selectivity but enhances Ca^{2+}/Mg^{2+} selectivity. Hence, Ca^{2+}/Na^+ selectivity is achieved when attractive Ca^{2+}−ligand electrostatic interactions in the pore prevail over unfavorable solvation effects (Figures 4a−c), consistent with previous works.[32,34,45,54,55,58,59,64,66] Our finding that the Ca^{2+}/Na^+ selectivity increases when the pore size decreases is also in line with previous studies.[45,56,59] In contrast, Ca^{2+}/Mg^{2+} selectivity is achieved in solvent-accessible channel pores, where solvation favors Ca^{2+} due to its smaller desolvation penalty compared to that of Mg^{2+}. The requirements for achieving Ca^{2+}/Mg^{2+} selectivity appear to be less stringent than those for attaining Ca^{2+}/Na^+ selectivity, as more filter structures are found to exhibit Ca^{2+}/Mg^{2+} selectivity (Figures 2−4, positive ΔG^x, $x > 10$) than Ca^{2+}/Na^+ selectivity (Figures 3a−c, positive ΔG^x, $x < 30$).

Among the various types of filters studied, a tetrameric filter lined by four carboxylates (**4COO$^-$**; EEEE/EEDD locus) is the only structure that selects Ca^{2+} over Na^+ and Mg^{2+} regardless of the solvent accessibility of the channel's pore; thus it seems to be the most discriminatory (Figure 5a, positive ΔG^x, $x \geq 4$). The larger **4COO$^-$/1W** or **3COO$^-$ + 1COOH** filters is Ca^{2+}-selective only if it is solvent-*accessible* (Figure 4c; positive ΔG^x, $x > 10$), whereas the **5CONH$_2$** filter is Ca^{2+}-selective only if it is solvent-*inaccessible* (Figure 3c; positive ΔG^x, $x < 4$). The other filters studied are either Na^+/Ca^{2+} selective (Figures 2, 3, and 4e, negative ΔG^x, $x > 4$) or are Ca^{2+}/Na^+ selective with severely compromised/reversed Ca^{2+}/Mg^{2+} selectivity (Figure 4a,c−e).

Na^+ Selectivity. The selectivity for monovalent Na^+ over divalent Ca^{2+}/Mg^{2+} is achieved when solvation effects, which favor Na^+, are stronger than the metal−ligand electrostatic interactions. Thus, the channel's selectivity for Na^+ over Ca^{2+}

and Mg^{2+} increases when the pore's solvent accessibility increases (enhancing solvation effects), but the number and charge-donating ability of the ligands lining the selectivity filter decreases (attenuating electronic effects). For selectivity filters lined with three or four weak charge-donating hydroxyl or backbone carbonyl groups, electronic effects are weak, so solvation effects dictate ion selectivity, favoring the cation with the smaller desolvation penalty; that is, Na^+ (Figures 2 and 3a,b). In particular, a solvent-exposed **3OH** filter is predicted to be highly selective for monovalent Na^+ compared to divalent Ca^{2+} or Mg^{2+} (Figure 2a). Interestingly, a EEEE filter can be Na^+-selective if it is solvent-accessible ($x > 30$) and either two or more acidic residues are protonated (Figure 4d,e) or bind the permeating metal cation indirectly via water molecules (Figure 5c,d).

Mg^{2+} Selectivity. Because Mg^{2+} is a stronger Lewis acid than Ca^{2+} or Na^+, electronic effects favor Mg^{2+} over Ca^{2+} or Na^+ in tri and tetrameric filters, but solvation effects reverse this preference and disfavor Mg^{2+} in solvent-exposed pores. The selectivity for Mg^{2+} over Ca^{2+} and Na^+ generally increases when the pore's solvent accessibility and oligomericity decreases, but the charge-donating ability of the ligands lining the selectivity filter increases. Hence solvent *inaccessible* trimeric filters lined by three Asp/Glu carboxylate groups (Figure 4a, **3COO$^-$**) might exhibit moderate Mg^{2+}/Ca^{2+} selectivity ($\Delta G^4 \sim 5$ kcal/mol), but high Mg^{2+}/Na^+ selectivity ($\Delta G^4 \sim 57$ kcal/mol). Another key factor controlling the selectivity for Mg^{2+} over Ca^{2+} or Na^+ is the pore size/rigidity. Whereas a EEEE pore fitting a bare or monohydrated metal cation is Ca^{2+}-selective (Figure 5a,b, positive ΔG^x, $x > 4$), a wider filter that can accommodate the metal bound to $\geq$2 water molecules may be Mg^{2+}-selective in a relatively low ($x \leq 10$) dielectric environment (Figure 5c,d).

Comparison with the Experiment. The results obtained are consistent with available experimental data. Notably, the degree of hydration of the native metal ion in its selectivity filter is consistent with the experimentally observed pore size and metal hydration state in the various types of ion channels.

Ca^{2+} Selectivity. Among a multitude of structures with different numbers and types of metal-ligating groups studied, the four-carboxylate locus was found to secure high selectivity for Ca^{2+} over both Na^+ and Mg^{2+}. This is consistent with the fact that four conserved EEEE/EEDD residues comprise the selectivity filters of the high/low voltage-activated Ca_v channels and the Ca^{2+} release-activated calcium channel,[98,99] which very efficiently discriminate between the "native" Ca^{2+} and competing Na^+ and Mg^{2+}. The unfavorable (positive) free energy for replacing Ca^{2+} bound to four carboxylates (**4COO$^-$**; Figure 4b) with Na^+ is also consistent with the observation that Ca^{2+} blocks Na^+ currents when it is already bound to the EEEE locus.[34] Figure 4 shows that the channel's selectivity for Ca^{2+} is enhanced if the Asp/Glu side chains from the EEEE/EEDD loci are deprotonated upon metal binding—this is in accord with experimental observations.[12,48] The results in Figure 5a,b predict that a relatively rigid EEEE selectivity filter with a constricted pore permeable to *dehydrated* or *mono*hydrated metal cations would be highly selective for Ca^{2+} over Na^+ and Mg^{2+}. Indeed, permeation experiments on various types of Ca^{2+}-selective Ca_v channels show selectivity filters that can accommodate a *bare* or *mono*hydrated metal cation.[100,101]

Na^+ Selectivity. The calculations predict that, in the absence of Ca^{2+}, a relatively rigid Ca^{2+}–selective **4COO$^-$** or **4COO$^-$/1W** filter would be selective for Na^+ over K^+, as it better fits Na^+ than the bulkier K^+ with diminished charge density. This is in accord with experiments showing that Ca^{2+}–free Ca_v channels exhibit high Na^+/K^+ selectivity.[7,102] Figures 5c,d show that a large, water-accessible EEEE selectivity filter that bind indirectly to cations via two or more water molecules would be Na^+-selective. These findings are in line with the X-ray structure of a Na^+-selective bacterial Na_v channel, which shows a large, water-filled EEEE selectivity filter that fits a metal cation bound indirectly to the Glu carboxylates via two in-plane water molecules.[10] The **4COO$^-$** filter (Figure 4b) becomes Na^+-selective upon mutation of the four carboxylates to amides (**4CONH$_2$**; Figure 3b)—this is in accord with the experimental finding that mutation of all four Glu residues comprising the EEEE filter in the high voltage-activated Ca_v channels to glutamine eliminates Ca^{2+} selectivity and significantly increases Na^+ permeability.[48] Not only is the **4CONH$_2$** (Figure 3b) Na^+-selective, but the **4OH** filter (Figure 2b) is also Na^+-selective. This agrees with the recent structure of the Na^+-selective Na_vRh bacterial channel showing four Ser residues lining the narrowest part of the pore.[103] Our finding that a trimeric filter lined by three Ser/Thr side chains is highly Na^+ selective (Figure 2a) is consistent with the *tri*meric structure found for an acid-sensing ion channel belonging to the epithelial Na^+ channel family.[15,16]

Limitations and Future Work. In this work, the architectural influence from the surrounding protein matrix and solvent was *implicitly* accounted by considering the effects of the protein matrix on (i) protonating one or more metal-ligating Asp/Glu residues (Figure 4), (ii) constraining the orientation of the metal ligands (Figure 6), and (iii) controlling the pore size and flexibility (Figure 5). When X-ray structures of metal-bound Ca_v or Na_v channels become available, the architectural influence from the surrounding protein matrix could be incorporated *explicitly* using all-atom free energy simulations or reduced models that incorporate the coupling between the metal ion and its ligands with the rest of the system.[104] The metal-bound Ca_v or Na_v channel structure would also enable free energy calculations to evaluate the contribution of the coupling between ions[105] and kinetic barriers[106] to ion selectivity in the selectivity filter as well as in other ion-binding sites in the channel pore.

■ CONCLUSIONS

This work reveals how the outcome of the competition between the native metal ion and its rival cations depends on the interplay between electronic and solvation effects. It also reveals how ion selectivity for the most selective ion-binding site in the narrowest region of the channel pore (i.e., the selectivity filter) depends on properties of the protein, the metal ligands, and the metal cation itself; namely,

(i) the protein's oligomericity, related to the number of the ligands lining the pore,
(ii) the pore's rigidity/size, which correlates with the degree of metal hydration inside the filter,
(iii) the pore's symmetry, constraining the ligands to bind the metal cation roughly in-plane,
(iv) the pore's solvent accessibility,
(v) the metal ligand's type/protonation state, and
(vi) the Ca^{2+} hydration number outside the filter.

The results show how changes in the composition and structure of the selectivity pore could favor one of the competing cations. Such changes may be quite subtle; for

example, the pore size (associated with the metal's degree of hydration in the selectivity filter) and the pore's solvent accessibility can "switch" selectivity filters lined with four carboxylates to be Ca^{2+}-, Mg^{2+}-, or Na^{+}-selective. The results, which are consistent with available experimental data on various types of ion channels, imply that, during the evolution, the selectivity filter of a given ion channel had been uniquely shaped in response to the specific physicochemical properties of the native metal ion, thus enabling it to select the native metal ion among rival cations from the surrounding fluids.

AUTHOR INFORMATION

Notes

The authors declare no competing financial interest.

ACKNOWLEDGMENTS

We thank Hanna Yuan for reading this work and helpful comments. This work was supported by Academia Sinica and the National Science Council, Taiwan (contract no. 95-2113-M-001-001 to C.L.).

REFERENCES

(1) Mano, I.; Driscoll, M. *Bioessays* **1999**, *21*, 568−578.
(2) Hille, B. *Ionic channels of excitable membranes*, 3rd ed.; Sinauer Associates: Sunderland, MA, 2001.
(3) Snyder, P. M. *Endocr. Rev.* **2002**, *23*, 258−275.
(4) Favre, I.; Moczydlowski, E.; Schild, L. *Biophys. J.* **1996**, *71*, 3110−3125.
(5) Schlief, T.; Schonherr, R.; Imoto, K.; Heinemann, S. H. *Eur. Biophys. J.* **1996**, *25*, 75−91.
(6) Hall, J. E. *Guyton and Hall Textbook of Medical Physiology with Student Consult Online Access*, 12th ed.; Elsevier Saunders: Philadelphia, 2011.
(7) Hess, P.; Lansman, J. B.; Tsien, R. W. *J. Gen. Physiol.* **1986**, *88*, 293−319.
(8) Heinemann, S. H.; Terlau, H.; Stuhmer, W.; Imoto, K.; Numa, S. *Nature* **1992**, *356*, 441−443.
(9) Backx, P. H.; Yue, D. T.; Lawrence, J. H.; Marban, E.; Tomaselli, G. F. *Science* **1992**, *257*, 248−251.
(10) Payandeh, J.; Scheuer, T.; Zheng, N.; Catterall, W. A. *Nature* **2011**, *475*, 353−359.
(11) Yue, L.; Navarro, B.; Ren, D.; Ramos, A.; Clapham, D. E. *J. Gen. Physiol.* **2002**, *120*, 845−853.
(12) Yang, J.; Ellinor, P. T.; Sather, W. A.; Zhang, J. F.; Tsien, R. W. *Nature* **1993**, *366*, 158−161.
(13) Koch, S. E.; Bodi, I.; Schwartz, A.; Varadi, G. *J. Biol. Chem.* **2000**, *275*, 34493−34500.
(14) Cibulski, S. M.; Sather, W. A. *J. Gen. Physiol.* **2000**, *116*, 349−362.
(15) Jasti, J.; Furukawa, H.; Gonzales, E. B.; Gouaux, E. *Nature* **2007**, *449*, 316−324.
(16) Canessa, C. M. *Nature* **2007**, *449*, 293−294.
(17) Doyle, D. A.; Cabral, J. M.; Pfuetzner, R. A.; Kuo, A.; Gulbis, J. M.; Cohen, S. L.; Cahit, B. T.; MacKinnon, R. *Science* **1998**, *280*, 69−67.
(18) Zhou, Y.; Morais-Cabral, J. H.; Kaufman, A.; MacKinnon, R. *Nature* **2001**, *414*, 43−48.
(19) Gouaux, E.; MacKinnon, R. *Science* **2005**, *310*, 1461−1465.
(20) Shi, N.; Ye, S.; Alam, A.; Chen, L.; Jiang, Y. *Nature* **2006**, *440*, 570−574.
(21) Jiang, Y.; Lee, A.; Chen, J.; Cadene, M.; Chait, B. T.; MacKinnon, R. *Nature* **2002**, *417*, 523−526.
(22) Kuo, A.; Gulbis, J. M.; Antcliff, J. F.; Rahman, T.; Lowe, E. D.; Zimmer, J.; Cuthbertson, J.; Ashcroft, F. M.; Ezaki, T.; Doyle, D. A. *Science* **2003**, *300*, 1922−1926.
(23) Jiang, Y.; Lee, A.; Chen, J.; Ruta, V.; Cadene, M.; Chait, B. T.; MacKinnon, R. *Nature* **2003**, *423*, 33−41.
(24) Long, S. B.; Tao, X.; Campbell, E. B.; MacKinnon, R. *Nature* **2007**, *450*, 376−382.
(25) Nishida, M.; Cadene, M.; Chait, B. T.; MacKinnon, R. *EMBO J.* **2007**, *26*, 4005−4015.
(26) Alam, A.; Jiang, Y. *Nat. Struct. Mol. Biol.* **2009**, *16*, 30−34.
(27) Eisenman, G. *Biophys. J.* **1962**, *2*, 259−323.
(28) Laio, A.; Torre, V. *Biophys. J.* **1999**, *76*, 129−148.
(29) Aqvist, J.; Luzhkov, V. *Nature* **2000**, *404*, 881−884.
(30) Luzhkov, V. B.; Aqvist, J. *Biochim. Biophys. Acta* **2001**, *1548*, 194−202.
(31) Noskov, S. Y.; Berneche, S.; Roux, B. *Nature* **2004**, *431*, 830−834.
(32) Corry, B.; Vora, T.; Chung, S.-H. *Biochim. Biophys. Acta* **2005**, *1711*, 72−86.
(33) Asthagiri, D.; Pratt, L. R.; Paulaitis, M. E. *J. Chem. Phys.* **2006**, *125*, 24701−1−6.
(34) Corry, B.; Chung, S.-H. *Cell. Mol. Life Sci.* **2006**, *63*, 301−315.
(35) Noskov, S. Y.; Roux, B. *Biophys. Chem.* **2006**, *124*, 279−291.
(36) Bostick, D. L.; Brooks, C. L., III. *Proc. Natl. Acad. Sci. U.S.A.* **2007**, *104*, 9260−9265.
(37) Thomas, M.; Jayatilaka, D.; Corry, B. *Biophys. J.* **2007**, *93*, 2635−2643.
(38) Varma, S.; Rempe, S. B. *Biophys. J.* **2007**, *93*, 1093−1099.
(39) Fowler, P. W.; Tai, K.; Sansom, M. S. P. *Biophys. J.* **2008**, *95*, 5062−5072.
(40) Varma, S.; Sabo, D.; Rempe, S. B. *J. Mol. Biol.* **2008**, *376*, 13−22.
(41) Dudev, T.; Lim, C. *J. Am. Chem. Soc.* **2009**, *131*, 8092−8101.
(42) Roux, B.; Berneche, S.; Egwolf, B.; Lev, B.; Noskov, S. Y.; Rowley, C. N.; Yu, H. *J. Gen. Physiol.* **2011**, *137*, 415−426.
(43) Dudev, T.; Lim, C. *J. Am. Chem. Soc.* **2010**, *132*, 2321−2332.
(44) Lodish, H. F. *Molecular Cell Biology*; Scientific American Books: New York, 1999.
(45) Boda, D.; Valisko, M.; Eisenberg, B.; Nonner, W.; Henderson, D.; Gillespie, D. *J. Chem. Phys.* **2006**, *125*, 034901−1−11.
(46) Kim, M. S.; Morii, T.; Sun, L. X.; Imoto, K.; Mori, Y. *FEBS Lett.* **1993**, *318*, 145−148.
(47) Tang, S.; Mikala, G.; Bahinski, A.; Yatani, A.; Varadi, G.; Schwartz, A. *J. Biol. Chem.* **1993**, *268*, 13026−13029.
(48) Ellinor, P. T.; Yang, J.; Sather, W. A.; Zhang, J. F.; Tsien, R. W. *Neuron* **1995**, *15*, 1121−1132.
(49) Parent, L.; Gopalakrishnan, M. *Biophys. J.* **1995**, *69*, 1801−1813.
(50) Bahinski, A.; Yatani, A.; Mikala, G.; Tang, S.; Yamamoto, S.; Schwartz, A. *Mol. Cell. Biochem.* **1997**, *166*, 125−134.
(51) Wu, X. S.; Edwards, H. D.; Sather, W. A. *J. Biol. Chem.* **2000**, *275*, 31778−31785.
(52) Perez-Reyes, E. *Physiol. Rev.* **2003**, *83*, 117−161.
(53) Nonner, W.; Eisenberg, B. *Biophys. J.* **1998**, *75*, 1287−1305.
(54) Nonner, W.; Catacuzzeno, L.; Eisenberg, B. *Biophys. J.* **2000**, *79*, 1976−1992.
(55) Eisenberg, B. *Biophys. Chem.* **2003**, *100*, 507−517.
(56) Boda, D.; Valisko, M.; Eisenberg, B.; Nonner, W.; Henderson, D.; Gillespie, D. *Phys. Rev. Lett.* **2007**, *98*, 168102−1−4.
(57) Boda, D.; Nonner, W.; Henderson, D.; Eisenberg, B.; Gillespie, D. *Biophys. J.* **2008**, *94*, 3486−3496.
(58) Boda, D.; Valisko, M.; Henderson, D.; Eisenberg, B.; Gillespie, D.; Nonner, W. *J. Gen. Physiol.* **2009**, *133*, 497−509.
(59) Malasics, A.; Gillespie, D.; Nonner, W.; Henderson, D.; Eisenberg, B.; Boda, D. *Biochim. Biophys. Acta* **2009**, *1788*, 2471−2480.
(60) Boda, D.; Giri, J.; Henderson, D.; Eisenderg, B.; Gillespie, D. *J. Chem. Phys.* **2011**, *134*, 055102.
(61) Giri, J.; Fonseca, J. E.; Boda, D.; Henderson, D.; Eisenberg, B. *Phys. Biol.* **2011**, *8*, 026004.
(62) Krauss, D.; Eisenberg, B.; Gillespie, D. *Eur. Biophys. J.* **2011**, *40*, 775−782.
(63) Corry, B.; Allen, T. W.; Kuyucak, S.; Chung, S.-H. *Biochim. Biophys. Acta* **2000**, *1509*, 1−6.
(64) Corry, B.; Allen, T. W.; Kuyucak, S.; Chung, S.-H. *Biophys. J.* **2001**, *80*, 195−214.

(65) Lipkind, G. M.; Fozzard, H. A. *Biochemistry* **2001**, *40*, 6786−6794.
(66) Ramakrishnan, V.; Henderson, D.; Busath, D. D. *Biochim. Biophys. Acta* **2004**, *1664*, 1−8.
(67) Dudev, T.; Lim, C. *Phys. Chem. Chem. Phys.* **2012**, DOI: 10.1039/C2CP00036A.
(68) Dudev, T.; Lim, C. *Chem. Rev.* **2003**, *103*, 773−787.
(69) Dudev, T.; Lim, C. *J. Chin. Chem. Soc.* **2003**, *50*, 1093−1102.
(70) Dudev, T.; Lim, C. *Acc. Chem. Res.* **2007**, *40*, 85−93.
(71) Dudev, T.; Lim, C. *Annu. Rev. Biophys.* **2008**, *37*, 97−116.
(72) Marcus, Y. *Chem. Rev.* **1988**, *88*, 1475−1498.
(73) Dudev, M.; Wang, J.; Dudev, T.; Lim, C. *J. Phys. Chem. B* **2006**, *110*, 1889−1895.
(74) Dudev, T.; Lim, C. *J. Phys. Chem. B* **2001**, *105*, 4446−4452.
(75) Babu, C. S.; Dudev, T.; Casareno, R.; Cowan, J. A.; Lim, C. *J. Am. Chem. Soc.* **2003**, *125*, 9318−9328.
(76) Dudev, T.; Lim, C. *J. Phys. Chem. B* **2004**, *108*, 4546−4557.
(77) Dudev, T.; Chang, L.-Y.; Lim, C. *J. Am. Chem. Soc.* **2005**, *127*, 4091−4103.
(78) Dudev, T.; Lim, C. *J. Am. Chem. Soc.* **2011**, *133*, 9506−9515.
(79) *GaussView 3.09*; Gaussian, Inc.: Pittsburgh, PA, 2000−2003.
(80) Frisch, M. J.; Trucks, G. W.; Schlegel, H. B.; Scuseria, G. E.; Robb, M. A.; Cheeseman, J. R.; Scalmani, G.; Barone, V.; Mennucci, B.; Petersson, G. A. et al. *Gaussian 09, Revision A.02*; Gaussian, Inc.: Wallingford, CT, 2009.
(81) Wong, M. W. *Chem. Phys. Lett.* **1996**, *256*, 391−399.
(82) Gilson, M. K.; Honig, B. *Proteins: Struct., Funct., Genet.* **1988**, *4*, 7−18.
(83) Lim, C.; Bashford, D.; Karplus, M. *J. Phys. Chem.* **1991**, *95*, 5610−5620.
(84) Bashford, D. An object oriented programming suite for electrostatic effects in biological molecules. In *Scientific Computing in Object-Oriented Parallel Environments*; Ishikawa, Y., Oldehoeft, R. R., Reynders, V. W., Tholburn, M., Eds.; Springer: Berlin, 1997; Vol. *1343*; pp 233−240.
(85) Dudev, T.; Lim, C. *J. Am. Chem. Soc.* **2006**, *128*, 1553−1561.
(86) Reed, A. E.; Curtiss, L. A.; Weinhold, F. *Chem. Rev.* **1988**, *88*, 899−926.
(87) Brooks, B. R.; Bruccoleri, R. E.; Olafson, B. D.; States, D. J.; Swaminathan, S.; Karplus, M. *J. Comput. Chem.* **1983**, *4*, 187−217.
(88) Smith, R. M.; Martell, A. E. *Sci. Total Environ.* **1987**, *64*, 125−147.
(89) Friedman, H. L.; Krishnan, C. V. Thermodynamics of ionic hydration. In *Water: A comprehensive treatise*; Franks, F., Ed.; Plenum Press: New York, 1973; Vol. 3; pp 1−118.
(90) Ben-Naim, A.; Marcus, Y. *J. Chem. Phys.* **1984**, *81*, 2016−2027.
(91) Chambers, C. C.; Hawkins, G. D.; Cramer, C. J.; Truhlar, D. G. *J. Phys. Chem.* **1996**, *100*, 16385−16398.
(92) Wolfenden, R. *Biochemistry* **1978**, *17*, 201−204.
(93) Shannon, R. D. *Acta Crystallogr., A* **1976**, *32*, 751−767.
(94) Glendening, E. D.; Feller, D. *J. Phys. Chem.* **1995**, *99*, 3060−3067.
(95) Glendening, E. D.; Feller, D. *J. Phys. Chem.* **1996**, *100*, 4790−4797.
(96) Chan, S. L.; Lim, C. *J. Phys. Chem.* **1994**, *98*, 692−695.
(97) Giesen, D. J.; Hawkins, G. D.; Liotard, D. A.; Cramer, C. J.; Truhlar, D. G. *Theor. Chem. Acc.* **1997**, *98*, 85−109.
(98) McNally, B. A.; Yamashita, M.; Engh, A.; Prakriya, M. *Proc. Natl. Acad. Sci. U.S.A.* **2009**, *106*, 22516−22521.
(99) Prakriya, M. *Immunol. Rev.* **2009**, *231*, 88−98.
(100) McCleskey, E. W.; Almers, W. *Proc. Natl. Acad. Sci. U.S.A.* **1985**, *82*, 7149−7153.
(101) Cataldi, M.; Perez-Reyes, E.; Tsien, R. W. *J. Biol. Chem.* **2002**, *277*, 45969−45976.
(102) Sather, W. A.; McCleskey, E. W. *Annu. Rev. Physiol.* **2003**, *65*, 133−159.
(103) Zhang, X.; Ren, W.; DeCaen, P.; Yan, C.; Tao, X.; Tang, L.; Wang, J.; Hasegawa, K.; Kumasaka, T.; He, J.; et al. *Nature* **2012**, *486*, 130−135.
(104) Roux, B. *J. Phys. Chem. B* **2012**, *116*, 6966−6979.
(105) Caplan, D. A.; Subbotina, J. O.; Noskov, S. Y. *Biophys. J.* **2008**, *95*, 4613−4621.
(106) Kim, I.; Allen, T. W. *Proc. Natl. Acad. Sci. U.S.A.* **2011**, *108*, 17963−17968.